

# GAMMA-RAY LINE OBSERVATIONS WITH RHESSI

David M. Smith

Department of Physics and Santa Cruz Institute for Particle Physics, University of California, Santa Cruz,  
1156 High Street, Santa Cruz, CA 95064 USA, dsmith@scipp.ucsc.edu

## ABSTRACT

The Reuven Ramaty High Energy Solar Spectroscopic Imager (RHESSI) has been observing gamma-ray lines from the Sun and the Galaxy since its launch in February 2002. Here I summarize the status of RHESSI observations of solar lines (nuclear de-excitation, neutron capture, and positron annihilation), the lines of  $^{26}\text{Al}$  and  $^{60}\text{Fe}$  from the inner Galaxy, and the search for positron annihilation in novae.

Key words: gamma rays; spectroscopy; nucleosynthesis; RHESSI.

## 1. INTRODUCTION

The *Reuven Ramaty High Energy Solar Spectroscopic Imager (RHESSI)*, which was launched on February 5, 2002, is part of NASA's Small Explorer series of satellites (Lin et al., 2002). *RHESSI* was designed to perform imaging and spectroscopy of solar flares in the hard x-ray and gamma-ray range, with both spatial and spectral resolution far superior to previous missions. It uses Rotating Modulation Collimators (RMCs) for solar imaging down to  $2.3''$  (Hurford et al., 2002). Its nine coaxial germanium detectors cover the range from 3 keV to 17 MeV with extremely good energy resolution ( $E/\Delta E$  around 400 from 1–2 MeV) (Smith et al., 2002). The detectors are in the rear of the spacecraft; the spacecraft bus is wrapped around the central tube that contains the optical axis. Each detector is segmented into a thin front segment, which records the copious hard x-ray photons from a solar flare, and a thick rear segment built to observe solar gamma-rays at higher energies that penetrate the front segment.

Only *RHESSI*'s coarsest grids are thick enough to effectively modulate gamma rays above 1 MeV. Imaging is therefore limited to  $35''$  at the 2.223 MeV line from neutron capture in solar flares, and to  $3'$  for the 4 and 6 MeV lines from carbon and oxygen

de-excitation. Solar spectroscopy can be performed across the entire energy range of the detectors, subject to the limitations of photon statistics at gamma-ray energies.

Because these detectors have no shielding, and because the spacecraft is very light, the *RHESSI* detectors can also see emission at gamma-ray energies from any direction in the sky. For photons on the order of 1 MeV or higher, in fact, the instrument's effective area (about  $29\text{ cm}^2$  at 1809 keV) has little dependence on the direction of incidence, with the exception of a  $\sim 30\%$  depression at near-solar angles due to the effects of the grids, absorption in the front segments, and opacity of parts of the spacecraft bus. Since *RHESSI* is in low-Earth orbit, the spectrum of emission from any given point in space can be derived by using the Earth as an occulter, subtracting blocked from unblocked data to determine background, if the source in question is the dominant source in the sky at the wavelength (and during the time period) under consideration.

## 2. SOLAR FLARE OBSERVATIONS

Observations of gamma-ray lines due to nuclear interactions in flares can help discriminate among models of ion acceleration. The data and the models meet in the intermediate terrain of the energy spectra, composition, location, and directivity of the accelerated ions: the gamma rays can be used to deduce these distributions and the models make varied predictions.

Much has been learned from these lines using scintillation detectors with moderate energy resolution, notably the Gamma-Ray Spectrometer on the Solar Maximum Mission (Share & Murphy, 1997, e.g.). With the advent of *RHESSI*, gamma rays in flares have been imaged with a spatial resolution comparable to the size of the emitting regions, and their spectra have been observed with high energy resolution for the first time (a feat that has now also been performed by *INTEGRAL* (Gros et al., 2004)).

A special volume of the *The Astrophysical Journal*

*Letters* presented a wide range of *RHESSI* results on the X4.8-class flare of 23 July, 2002, a copious emitter of gamma rays. Figure 1 shows the lightcurve of the flare in several energy bands. Figure 2 shows an overview of the spectrum across *RHESSI*'s range of coverage. The results reported in that volume are summarized in Lin et al. (2003), and include:

- The discovery (Hurford et al., 2003) that the 2.223 MeV neutron-capture line in this flare, a good tracer of the interactions of accelerated ions, was centered at a position significantly offset from the distribution of hard x-rays from electron bremsstrahlung. The spatial separation between accelerated ions and electrons in this flare puts strong constraints on acceleration models.
- The unexpectedly large width ( $8.1 \pm 1.1$  keV) of the positron-annihilation line (Share et al., 2003a). Two possible local conditions could prevail to give a line this broad: a very high-temperature yet dense and extended plasma of  $(4-7) \times 10^5$  K, or a similarly extensive plasma at a temperature restricted to a very narrow range around 6000 K. Neither environment is expected to be typical of flaring atmospheres, but little is known about their true conditions.
- Significant redshifts and broadening found in the nuclear de-excitation lines of C, O, Ne, Mg, Si, and Fe (Smith et al., 2003a). These Doppler effects are due to gamma emission while the nucleus is still recoiling from a collision, and have been observed before (Share & Murphy, 1997), but not with high energy resolution. The redshifts were unexpectedly high for a flare on the solar limb, suggesting either a magnetic loop tilted toward the observer or an extreme beaming of the ions toward the solar surface (but see below).
- A very broad shape for the lines from interactions of accelerated  $\alpha$  particles with ambient  $^4\text{He}$  (Share et al., 2003b). These lines (from  $^7\text{Be}$  at 429 keV and  $^7\text{Li}$  at 478 keV) combine to make a single broad peak of characteristic shape, indicating that the angular distribution of the accelerated particles was **not** beamed.
- A study, using an advanced model of ion propagation in magnetic loops, of the time delay of the neutron capture line compared to prompt nuclear emissions (Murphy et al., 2003). The conclusion was that pitch-angle scattering of the ions must be taking place in the coronal part of the loop.

Work currently in progress includes a study (Shih et al., 2004) of variability of line ratios between the two halves of this flare (marked in Figure 1), and extensive studies of the gamma-ray emission in the large X-class flares of October/November 2003.

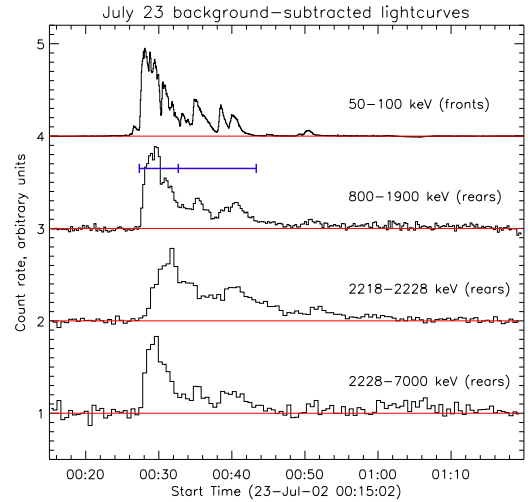


Figure 1. Background-subtracted *RHESSI* lightcurves of the X4.8 flare of 23 July, 2002. The top plot shows the hard x-rays from electron bremsstrahlung, and the other three channels are dominated by gamma rays from nuclear interactions of accelerated ions. The third plot is the lightcurve of the narrow line from neutron capture at 2.223 MeV, showing the delay due to the neutron thermalization time.

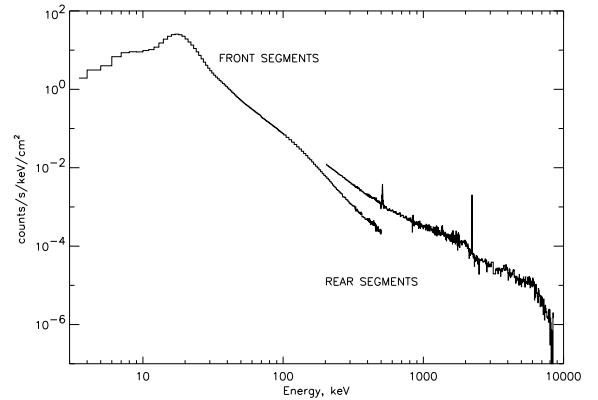


Figure 2. The broad-band count spectrum of the flare of 23 July, 2002 as observed with *RHESSI*, demonstrating the extremely large dynamic range of the instrument in both energy and flare flux (*RHESSI* has also usefully studied microflares over five orders of magnitude smaller than this event). The positron-annihilation line at 511 keV and the neutron capture line at 2.223 MeV are clearly visible, as is the cutoff above 7 MeV where there is no longer a strong contribution from nuclear lines. The decline below 20 keV is due to aluminum attenuators that are moved in front of the detectors to control the count rate in bright flares.

### 3. GALACTIC NUCLEOSYNTHESIS

#### 3.1. $^{26}\text{Al}$

The radioactive lines from  $^{26}\text{Al}$  and  $^{60}\text{Fe}$  were extracted for the inner Galaxy, a region defined as covering  $\pm 30^\circ$  in Galactic longitude and  $\pm 5^\circ$  in Galactic latitude. When *none* of this region was occulted by the Earth, each minute of data was summed into the total "source" spectrum, and when *all* of it was occulted, the spectrum was used to create a database of background spectra. Similar background subtraction techniques have been used for observations with the *Solar Maximum Mission* Gamma-Ray Spectrometer (*SMM/GRS*) (Harris et al., 1990; Harris, Share, & Leising, 1994) and the Burst And Transient Source Experiment on the *Compton Gamma-Ray Observatory* (Smith et al., 1996a,b).

Although the fluxes thus derived have virtually no dependence on the distribution of the isotopes *within* the inner Galaxy box, the distribution *outside* will affect the recorded flux in a complicated way, depending on whether it resides in parts of the sky more often appearing in source or background spectra. This issue is being studied in detail by Wunderer et al. (2004).

I reported the  $^{26}\text{Al}$  flux for the first nine months of the *RHESSI* mission to be  $(5.71 \pm 0.54) \times 10^{-4}$  ph cm $^{-2}$  s $^{-1}$  (Smith, 2003, 2004), comparable to the value found by the GRIS balloon (Naya et al., 1996) but significantly higher than the sum of the COMPTEL map in this range of Galactic longitude (Diehl et al., 1995). I have recently discovered a significant error in the calculation of the instrumental effective area, however. The correct effective area, taking a weighted average over all the angles of incidence during the different pointing periods used, should have been 29.3 cm $^2$  rather than the 20.5 cm $^2$  quoted earlier. The initial result should then have been  $(3.99 \pm 0.38) \times 10^{-4}$  ph cm $^{-2}$  s $^{-1}$ , in much better agreement with the results from COMPTEL and other instruments. The results below and in the future will use the correct instrumental response. With minor improvements to the data selection and background selection algorithms since Smith (2003), I now find  $(3.89 \pm 0.36) \times 10^{-4}$  ph cm $^{-2}$  s $^{-1}$  for the same data set; the change other than that due to the instrument effective area is negligible.

The later data set (Figure 3, middle panel) gives a flux of only  $(3.03 \pm 0.36) \times 10^{-4}$  ph cm $^{-2}$  s $^{-1}$  when fit, as the first data set was, with a simple Gaussian. It is clear, however, from the shape of the line, that there is a significant tailing of the line shape due to radiation damage in the detectors as the mission progresses. This tailing is more obvious and more quantifiable in the background lines, which can be accumulated with extremely small error bars over long time intervals. By studying these lines, particularly the line of  $^{40}\text{K}$  (which will have a constant flux throughout the mission since it is a natural radioactivity), we can determine the effect

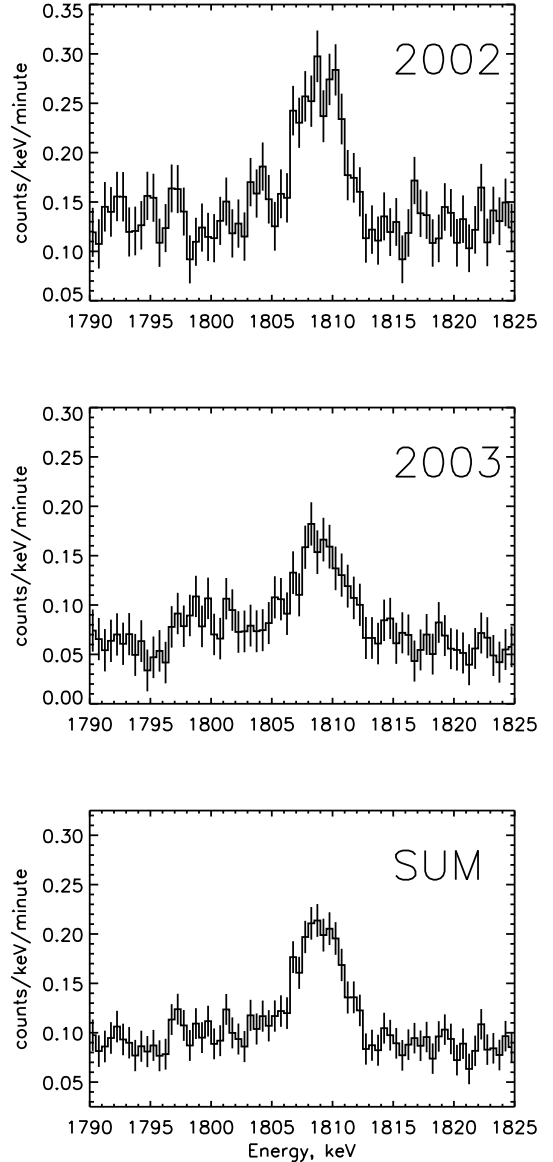


Figure 3. 1809 keV line profiles for the early mission (2002 March–November), the later mission (2002 December – 2003 November) and the sum of the two periods. Radiation damage in the detectors adds a tail to the line shape and degrades the photopeak response, and this effect increases with time.

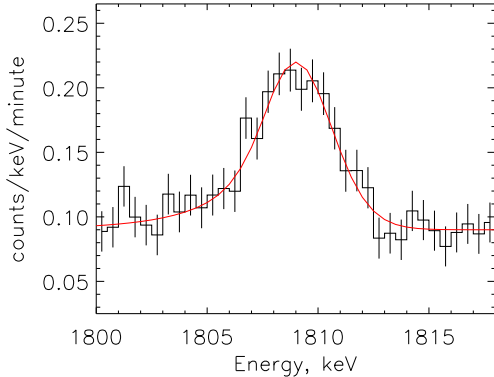


Figure 4. The 1809 keV profile for the whole mission with the instrumental lineshape superimposed. It is clear that there is no significant broadening beyond the instrumental response.

that radiation damage has on the measured flux for a Gaussian fit. This correction, based on the data, has also been checked with simulations (these simulations were made before the start of the mission and have accurately predicted the degree of radiation damage versus time). The corrected flux for the later data set is  $(3.46 \pm 0.41 \pm 0.18) \times 10^{-4} \text{ ph cm}^{-2} \text{ s}^{-1}$ , where the second error listed is a generous margin for systematic errors in the radiation-damage correction. The corrected value is compatible within statistical errors with the measurement from the first year.

The summed data set for the entire mission to date gives  $(3.35 \pm 0.24) \times 10^{-4} \text{ ph cm}^{-2} \text{ s}^{-1}$  uncorrected, and  $(3.69 \pm 0.27 \pm 0.11) \times 10^{-4} \text{ ph cm}^{-2} \text{ s}^{-1}$  corrected for radiation damage. The effective area for the full data set is slightly lower ( $28.6 \text{ cm}^2$ ), since it includes a December/January period when the Galactic Center is near the Sun. Now that the effective area has been corrected, the *RHESSI* data no longer support the tentative conclusion (Naya et al., 1998), based on the GRIS balloon data, that there might be a low-surface-brightness, highly diffuse component of the 1809 keV line not visible to imaging instruments like COMPTEL. Rather, they are now consistent with the results from COMPTEL and *SMM*/GRS Harris et al. (1990), another wide-field instrument like GRIS and *RHESSI*.

The GRIS result also included a measurement of the intrinsic line width (i.e. with instrumental broadening removed) that was surprisingly broad ( $5.4 (+1.4, -1.3) \text{ keV}$ ) (Naya et al., 1996), which was difficult to understand theoretically, since supernova ejecta come to rest in the interstellar medium on a timescale much shorter than the half-life of  $^{26}\text{Al}$ . The *RHESSI* result for the intrinsic width in the first nine months of the mission was  $2.03 (+0.78, -1.21) \text{ keV}$ , in clear disagreement with GRIS and consistent with the  $\sim 1 \text{ keV}$  width expected from Galactic rotation (Kretschmer et al., 2003). Including the data through 2003 November, I find  $0.9 (+1.1, -0.9) \text{ keV}$ . Figure 4 shows the line shape (also shown in

the bottom panel of Figure 3, with the instrumental line shape superimposed. The instrumental shape, which has a full width at half maximum of  $4.5 \text{ keV}$  and a significant low-energy tail, was derived from background lines at nearby energies.

### 3.2. $^{60}\text{Fe}$

The radioactivity of Galactic  $^{60}\text{Co}$ , the daughter of  $^{60}\text{Fe}$ , which is expected to be produced in core-collapse supernovae that may also produce much of the Galactic  $^{26}\text{Al}$ , has not previously been observed. Lines are expected at  $1173 \text{ keV}$  and  $1332 \text{ keV}$  with equal intensity. Models of nucleosynthesis have predicted that the ratio of the  $^{60}\text{Fe}/^{26}\text{Al}$  lines from the population of Galactic supernovae is on the order of 15% (Timmes et al., 1995), but higher ratios have also been calculated more recently (Rauscher et al., 2002; Limongi & Chieffi, 2003), leading to a renewal of the suggestion that supernovae may not be the dominant source of  $^{26}\text{Al}$  (Prantzos, 2004).

An analysis of the first 14 months of *RHESSI* data (Smith, 2004), which combined the two lines to increase the statistical significance of the result, found a flux per line of  $(16 \pm 5)\%$  of the 1809 keV flux. This analysis was similar to that performed for the 1809 keV line, except that data shortly after passes through the South Atlantic Anomaly (SAA) were removed due to the presence of an SAA-activated line, probably from  $^{60}\text{Cu}$ , at  $1332 \text{ keV}$ . Summing the data through November 2003, using an improved algorithm to better identify SAA-contaminated periods, and using corrected instrumental effective areas at both energies, the ratio is now found to be  $(9.7 \pm 3.9)\%$ . Most of the difference is due to the incorporation of new data rather than the changes in the analysis method (the error in effective areas was comparable at both energies). The radiation-damage correction is significantly less important at these energies than at  $1809 \text{ keV}$  and has not been applied. Figure 5 shows the individual lines and their sum. The  $1173 \text{ keV}$  line has a significance of only  $1.4\sigma$ , with a flux of  $(2.8 \pm 2.0) \times 10^{-5} \text{ ph cm}^{-2} \text{ s}^{-1}$ , and the  $1332 \text{ keV}$  line has a flux of  $(4.2 \pm 1.7) \times 10^{-5} \text{ ph cm}^{-2} \text{ s}^{-1}$  ( $2.4\sigma$ ), giving an average of  $(3.6 \pm 1.4) \times 10^{-5} \text{ ph cm}^{-2} \text{ s}^{-1}$  ( $2.6\sigma$ ). Further data will be added as the mission progresses.

### 3.3. Positron Annihilation in Novae

Models of classical novae from either CO or ONe white dwarfs predict copious emission in the positron annihilation line at  $511 \text{ keV}$  from radioactive decay of  $^{13}\text{N}$  and  $^{18}\text{F}$ , starting at the moment of explosion (Hernanz & José, 2004). This emission occurs long before the nova could be detected in visible light, so an instrument that views a substantial portion of the sky is required to detect this emission. So far, only upper limits have been obtained, from BATSE on *CGRO* (Hernanz et al., 2000) and TGRS

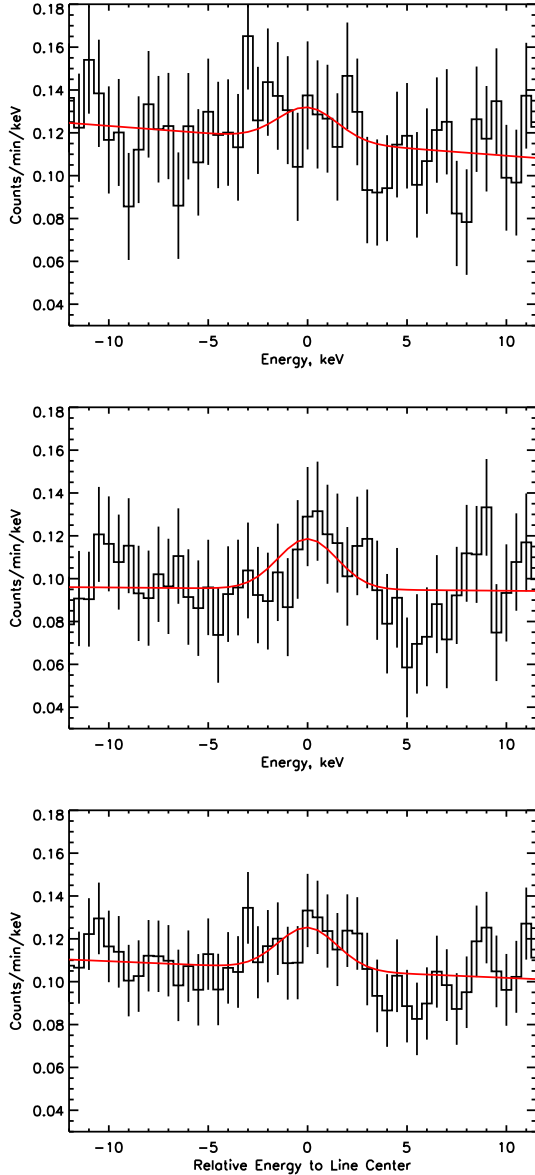


Figure 5. The 1173 keV (top) and 1332 keV (middle) profiles for the whole mission, and their sum (bottom), shifted to put the expected line center at zero energy.

on *Wind* (Harris et al., 1999, 2000). Both studies obtained upper limits on the annihilation line from  $^{18}\text{F}$ , which has a duration on the order of half a day. The  $3\sigma$  upper limits on individual novae averaged  $2.4 \times 10^{-3} \text{ ph cm}^{-2} \text{ s}^{-1}$  over 6-hour intervals with TGRS (Harris et al., 1999) and  $2.1 \times 10^{-3} \text{ ph cm}^{-2} \text{ s}^{-1}$  over 12-hour intervals with BATSE. Despite the TGRS detector having only a tiny fraction of BATSE’s area, it was able to reach comparable sensitivity due to its high energy resolution, since the high velocity of the nova ejecta would give a blueshift to the material on the near side of the white dwarf, moving the line a few keV away from the bright background line. *RHESSI* has comparable energy resolution and nearly an order of magnitude more detector volume than TGRS, but its background level is about a factor of two higher due to the proximity of the Earth. Thus we expect *RHESSI* to have between a factor of 2 and 2.5 better sensitivity for this measurement than TGRS and BATSE.

Since those limits were published, better laboratory data and modeling have resulted in new predictions that the line from  $^{18}\text{F}$  will be considerably lower than previously thought, putting it beyond the sensitivity of *RHESSI* and requiring either a very serendipitous detection by *INTEGRAL*/SPI in its field of view, or else the launch of a future, highly sensitive mission with full-sky or nearly full-sky coverage such as NASA’s planned Black Hole Finder Probe and Advanced Compton Telescope (ACT). These newer estimates (Hernanz & José, 2004; Kudryashov et al., 2000) also predict, however, that the line from  $^{13}\text{N}$ , lasting only for the first couple of hours of the explosion, could be much brighter, particularly for CO novae, and could therefore present a good target for *RHESSI*; it is also expected, by virtue of appearing earlier, to have a higher redshift.

Although there has not been any particularly close nova since *RHESSI*’s launch, the month of September 2002 provided two distant novae in the direction of Sagittarius (Liller et al., 2002; Haseda et al., 2002). Figure 6 shows *RHESSI* spectra in two hour accumulations from September 1–24, a period that almost certainly contains the outbursts from both novae. Background has been subtracted by using data 15 orbits (almost exactly one day) ahead and behind the interval of interest. This provides good subtraction to a level of a few percent, but the Figure shows that even this results in very large residuals at the unshifted annihilation line. Superimposed on the data in Figure 6 is *RHESSI*’s response to a blueshifted annihilation line at a flux level of  $0.01 \text{ photons cm}^{-2} \text{ s}^{-1}$ , equivalent to some of the brighter predictions (Hernanz & José, 2004; Kudryashov et al., 2000) for a distance of 1 kpc; this is intended more to give a notion of what could be observed from a closer event than to represent an expected signal from these particular novae.

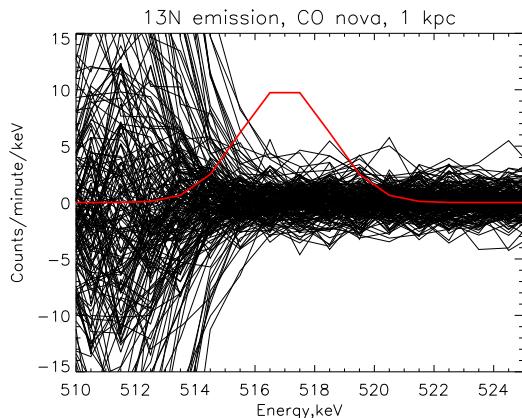


Figure 6. Background-subtracted 2-hour count spectra (see text) for 1–24 September 2002. Note the large background variability at the unshifted 511 keV line. For comparison, a blueshifted line is shown at  $0.01 \text{ photons cm}^{-2} \text{ s}^{-1}$ , an optimistic estimate for  $^{13}\text{N}$  production in a CO nova at 1 kpc.

#### 4. FUTURE WORK

All of the studies described here are ongoing. We are currently studying the lines from the flares of October/November 2003 and making plans for other solar studies, including a search for steady ion acceleration by studying the quiet Sun for low-level line emission and a search for radioactive  $^{56}\text{Co}$  in the aftermath of large flares (Ramaty & Mandzhavidze, 2000). The study of the  $^{26}\text{Al}$  line is bringing us together with *INTEGRAL*/SPI to combine the information at different spatial scales (Wunderer et al., 2004), and the  $^{60}\text{Fe}$  result is simply awaiting the gradual accumulation of further data. We will survey the entire sky for flashes of annihilation radiation (from classical novae or any other source), as has been done with other instruments (Harris et al., 2000; Smith et al., 1996a; Cheng et al., 1998). Finally, we will use the same technique that was used for the Galactic center lines to see if we can obtain a high-resolution measurement of the 1157 keV line from  $^{44}\text{Ti}$  in the Cas A supernova remnant.

#### ACKNOWLEDGMENTS

This work is supported by NASA contract NAS5-98033.

#### REFERENCES

Cheng, L. et al. (1998), *ApJ*, 503, 809  
 Diehl, R. et al. (1995), *A&A*, 298, 445  
 Gros, M. et al. (2004), this volume  
 Harris, M. J. et al. (1990), *ApJ*, 362, 135  
 Harris, M. J., Share, G. H., & Leising, M. D. (1994), *ApJ*, 433, 87

Harris, M. J. et al. (1999), *ApJ*, 522, 424  
 Harris, M. J. et al. (2000), *ApJ*, 542, 1057  
 Haseda, K. et al. (2002), *IAUC* 7975  
 Hernanz, M. J. et al. (2000), *Proceedings of the 5th Compton Symposium*, AIP Conf. Proc. 510, 82  
 Hernanz, M. J. & José, J. (2004), *New Ast. Rev.*, 48, 35  
 Hurford, G. J. et al. (2002), *Solar Physics*, **210**, 61  
 Hurford, G. J. et al. (2003), *ApJL*, 595, L77  
 Kretschmer, K., Diehl, R., & Hartmann, D. H. (2003), *A&A*, 412, L47  
 Kudryashov, A. D., Chugai, N. N., & Tutukov, A. V. (2000), *Ast. Rep.* 44, 170  
 Liller, W. et al. (2002), *IAUC* 7971  
 Limongi, M. & Chieffi, A. (2003), *ApJ*, 592, 404  
 Lin, R. P. et al. (2002), *Solar Physics*, **210**, 3  
 Lin, R. P. et al. (2003), *ApJL*, 595, L69  
 Murphy, R. J. et al. (2003), *ApJL*, 595, L93  
 Naya, J. E. et al. (1996), *Nature*, 384, 44  
 Naya, J. E. et al. (1998), *ApJL*, 499, L169  
 Prantzos, N. (2004), *astro-ph/0402198*, accepted in *A&A*  
 Ramaty, R. & Mandzhavidze, N. (2000), *Highly Energetic Physical Processes and Mechanisms for Emission from Astrophysical Plasmas*, Proc. IAU Symp. #195, 123  
 Rauscher, T. et al. (2002), *ApJ*, 576, 323  
 Share, G. H. et al. (2003), *ApJL*, 595, L85  
 Share, G. H. et al. (2003), *ApJL*, 595, L89  
 Share, G. H. & Murphy, R. J. 1997, *ApJ*, 485, 409  
 Shih, A. Y. et al. (2004), in preparation  
 Smith, D. M., et al. (1996a), *ApJ*, 471, 783  
 Smith, D. M., et al. (1996b), *A&AS*, 120, 361  
 Smith, D. M. et al. (2002), *Solar Physics*, **210**, 33  
 Smith, D. M. et al. (2003), *ApJL* 595, L81  
 Smith, D. M. (2003), *ApJL*, 589, L55  
 Smith, D. M. (2004), *New Ast. Rev.*, 48, 89  
 Timmes, F. X., et al. (1995), *ApJ*, 449, 204  
 Wunderer, C. et al. (2004), this volume